# Quantum bubble defects in the lowest-Landau-level crystal

Alexander C. Archer and Jainendra K. Jain

*Department of Physics, 104 Davey Lab, The Pennsylvania State University, University Park, Pennsylvania 16802, USA*

A longstanding puzzle for the lowest-Landau-level crystal phase has been an order of magnitude discrepancy between the theoretically calculated energy of the defects and the measured activation gap. We perform an extensive study of various kinds of defects in the correlated composite fermion crystal and find that the lowest energy defect is a sixfold symmetric "hypercorrelated bubble interstitial," in which an interstitial particle forms a strongly correlated bound state with a particle of the crystal. The energy of the bubble defect is a factor of $\sim$3 smaller than that of the lowest energy defect in a Hartree-Fock crystal. The anomalously low activation energies measured in transport experiments are thus a signature of the unusual quantum nature of the crystal and its defects.

PACS number(s): 73.43.−f, 71.10.Pm

When the extent of the quantum mechanical wave function of particles localized at the lattice sites of a crystal is comparable to the lattice constant, quantum mechanical effects can produce qualitatively new behavior. That has inspired fascinating developments in the contexts of $^3$He and $^4$He solids [1], as well as a longstanding interest in the crystal of electrons in the lowest Landau level (LLL) of a two-dimensional electron system (2DES) where the lattice constant is comparable to the magnetic length that governs the size of the electron wave packet. (In contrast, for the electron crystal on the surface of liquid helium [2], the quantum nature of electrons plays no measurable role.) The insulating phase observed at low fillings of the LLL [3–14] is believed to be a pinned crystal, and it is natural to ask in what ways the quantum nature of this crystal manifests in measurements. We show in this Rapid Communication that a striking feature of this crystal is the appearance of an unusual, nonclassical defect with an extremely low energy.

Surprisingly little theoretical work has been performed to investigate the lowest energy defects of the LLL crystal, even though it was deduced experimentally more than two decades ago from the activated behavior of the longitudinal resistance $\rho_{xx} \propto e^{\Delta/k_B T}$ in the insulating phase. The theoretical energies of various defects in a Hartree-Fock (HF) crystal, shown below, are found to be roughly an order of magnitude larger, thus indicating that the HF crystal is not a good description of the actual state. Indeed, theoretical work has shown that a crystal of composite fermions [15–19] is superior to a HF crystal of electrons, and is also very close to the crystal formed in exact diagonalization studies [17]. Electrons thus take advantage of both the composite fermion (CF) and the crystal correlations to seek the lowest energy state: They bind fewer than the maximal number of vortices available to them and use the remaining degrees of freedom to form a crystal. We consider several point defects of the triangular CF crystal (CFC) and find the striking result that the lowest energy defect is not one of the standard point defects (i.e., a vacancy, an edge interstitial, or a centered interstitial) but rather a sixfold symmetric interstitial that we call a "bubble interstitial," depicted in Fig. 1(a), in which the interstitial composite fermion forms a strongly correlated liquid bubble with one of the composite fermions forming the crystal; such a defect is not captured by elasticity theory because of its short range correlations. Furthermore, the CF bubble defect has a substantially lower energy than the

lowest energy defect in the HF crystal. That leads us to suggest that the anomalously low energy of defects as deduced by transport experiments is a signature of the correlated quantum mechanical nature of the LLL crystal as well as its defects.

We define the defect energy $E_\mathrm{D}$ as [20]

$$E_\mathrm{D} = \lim_{N \to \infty} \left( E_\mathrm{def}^{(N)} - E_0^{(N)} \right), \tag{1}$$

where $E_\mathrm{def}^{(N)}$ is the energy of an $N$ particle crystal containing a defect and $E_0^{(N)}$ is the energy of a defect-free $N$ particle crystal. These energies include the interaction with the background and are evaluated at constant density (i.e., equal area). We find a smoother behavior as a function of $N$ by using the relation

$$E_\mathrm{D} = \lim_{N \to \infty} \left( \frac{N}{N \pm 1} E_\mathrm{def}^{(N \pm 1)} - E_0^{(N)} \right), \tag{2}$$

because the lattice away from the defect is minimally changed between the crystals with and without defect.

We perform our calculations in the spherical geometry [21]. We form crystals on the surface of a sphere by placing wave packets at the Thomson minimum locations [22,23] determined by minimizing the energy of $N$ charged point particles on the sphere. The sites are generally sixfold co-ordinated, although the presence of some disclination defects is unavoidable in this geometry. The microscopic coordinates are denoted by $r_j = (\theta_j, \phi_j)$ and the electron sites are denoted by $R_l = (\gamma_l, \delta_l)$ in terms of the polar and the azimuthal angles. When describing the wave functions, it is convenient to use the spinor notation $(u_j, v_j) = [\cos(\theta_j/2)e^{i\phi_j/2}, \sin(\theta_j/2)e^{-i\phi_j/2}]$ and $(U_l, V_l) = [\cos(\gamma_l/2)e^{i\delta_l/2}, \sin(\gamma_l/2)e^{-i\delta_l/2}]$. We create a vacancy or an interstitial by removing a particle from a lattice site or by adding a particle to an interstitial site. Edge interstitial sites are given by $R_\mathrm{edge} = (R_1 + R_2)/|R_1 + R_2|$ and centered interstitial sites are given by $R_\mathrm{centered} = (R_1 + R_2 + R_3)/|R_1 + R_2 + R_3|$, where $R_1$, $R_2$, and $R_3$ are any three neighboring lattice sites. A bubble interstitial [24,25] in a HF (CF) crystal consists of an electron (CF) pair localized at a Thomson lattice site.

Relaxing the crystal lattice around a defect is crucial for obtaining realistic defect energies. Past techniques for calculating the defect energy [20,26,27] rely on a periodic repetition of a large unit cell, and are not appropriate for use in the spherical geometry. One must also take care not to relax the lattice by minimizing the energy of the entire
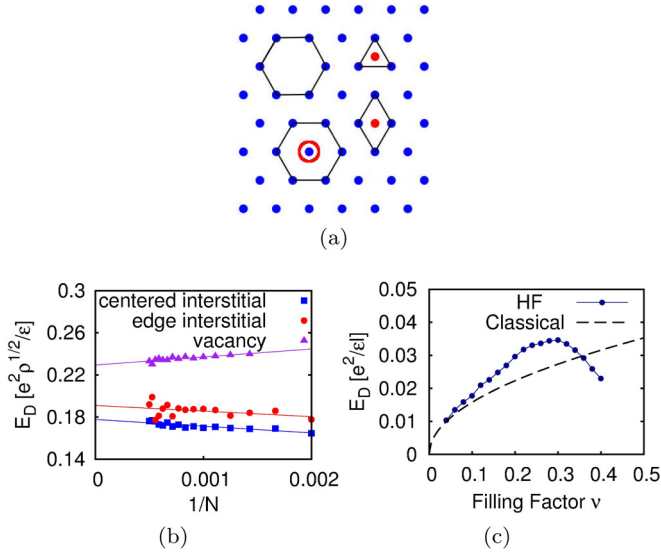
FIG. 1. (Color online) (a) A schematic representation of the defect configurations that we have considered. A vacancy is shown on the top left. Going clockwise, the other three defects are centered, edge, and bubble interstitials (with the added particle shown in red). The vacancy and the bubble interstitial have sixfold symmetry, whereas the centered and edge interstitials have threefold and twofold symmetry, respectively. (b) The energies of various defects in a classical crystal, calculated using the radial relaxation procedure only, as a function of the system's size on the sphere. (c) The energy of the fully relaxed edge interstitial defect for the LLL Hartree-Fock (HF) crystal (solid circles) and the classical crystal of point charges (dashed line) as a function of filling factor.

system since this will simply heal the defect and produce a Thomson crystal with one more or fewer composite fermions. We have developed an efficient method for calculating the defect energy that proceeds along the following steps. We place the defect far from native disclinations on the sphere and first carry out "radial relaxation" which consists of a series of cycles during each of which we systematically allow successive sets of the defect's nearest neighbors to move either away from or toward the defect until the lowest energy is obtained. We find that for the system sizes considered here, the first relaxation cycle is the most important for the classical and HF crystals, reducing the defect energy by ∼70% for a vacancy and ∼85% for an interstitial; subsequent cycles produce a relatively small further reduction of 1%–2% for a vacancy and within ∼5% for an interstitial. Radial relaxation alone cannot be expected to produce the lowest possible defect energies, however. The complete relaxation procedure consists of relaxing the defect's first through fifth nearest neighbors using the conjugate gradient method [20] (we found no further energy reduction by going to farther neighbors), relaxing the remainder of the lattice using radial relaxation, and obtaining the final defect energy by extrapolating to the thermodynamic limit. We have tested the effectiveness of this relaxation procedure by calculating defect energies for classical and LLL HF crystals (details below), where point charges interact through the Coulomb or the Maki-Zotos (MZ) interaction [28] [the MZ interaction $V_{MZ} = \sqrt{\pi} I_0(r^2/8)\text{sech}(r^2/8)/4$, where $I_0$ is the modified Bessel function, gives the Coulomb

interaction energy between two Gaussian wave packets in the LLL] for system containing up to $N = 2000$ particles. For a fixed filling factor in the spherical geometry, the density of a system has a slight $N$ dependence; the effect of this variation can be eliminated by making the "density correction" to total energy by multiplying it by a factor of $\sqrt{2Q\nu/N}$, which improves convergence of our results to the thermodynamic limit; we make this correction in all results. We plot the defect energies for classical systems calculated using radial relaxation in Fig. 1(b) and the fully relaxed classical and HF edge interstitial defect energy in Fig. 1(c). The energies of a classical crystal in zero magnetic field are expressed in units of $e^2\sqrt{\rho}/\epsilon$ and those for the LLL crystal in units of $e^2/\epsilon\ell$, where $\ell = \sqrt{\hbar c/eB}$ is the magnetic length. We find that the classical defect energies calculated using this method are consistent with those found in previous studies [20,26,27], producing centered and edge interstitial defect energies of 0.125, and 0.19 for the vacancy defect. Comparison with Fig. 1(b) indicates that radial relaxation alone is not satisfactory, especially for the interstitials. The lowest energy defects for both classical and HF systems are interstitials, with there being only a small difference between the edge and the centered interstitial. We note that the HF defect has significantly higher energy than the corresponding classical defect for the filling factor range of interest [Fig. 1(c)].

We now proceed to describe the crystal and defect wave functions for composite fermions. To construct the wave function for the defect-free CFC of composite fermions carrying $2p$ vortices, denoted $^{2p}$CFC, we place wave packets of electrons, $\phi_{R_l}^{2Q^*}(r_m) = (\widetilde{U}_l u_m + \widetilde{V}_l v_m)^{2Q^*}$, at the Thomson minimum locations [23], where $2Q^*$ is the effective monopole strength; antisymmetrize the product; and then composite-fermionize by attaching $2p$ vortices to each particle [29,30]. The final wave function is given by

$$\Phi_{2Q,\{R\}}^{2p} = \prod_{j<k}^{N}(u_j v_k - v_j u_k)^{2p} A\left(\prod_{1\leqslant j\leqslant N} \phi_{R_j}^{2Q^*}(r_j)\right), \quad (3)$$

where $N$ is the number of particles, the monopole strength is $2Q = 2Q^* + 2p(N-1)$, $\{R\} \equiv \{R_1, R_2, \ldots, R_N\}$ denotes the Thomson lattice sites, and $A$ is the antisymmetrization operator.

The wave function for an unrelaxed vacancy is identical to that of the $N$ particle CFC except that a single lattice site is left unoccupied. For an unrelaxed interstitial, we insert an additional CF at $R_I$. Following Zheng and Fertig [31], we also consider a "hypercorrelated" interstitial in which we attach $q$ extra vortices to the interstitial defect to build in additional repulsive correlations with the surrounding lattice. The resulting interstitial wave function is given by

$$\Phi_{2Q,\{R\},R_I}^{2p,q} = \prod_{j<k}^{N+1}(u_j v_k - v_j u_k)^{2p}$$

$$\times A\left((J_1)^q \phi_{R_I}^{2Q'}(r_1) \prod_{1\leqslant j\leqslant N} \phi_{R_j}^{2Q''}(r_{j+1})\right), \quad (4)$$

where $J_j = \prod_{k \neq j}(u_j v_k - v_j u_k)$, $2Q' = 2Q^* - q(N-1)$, $2Q'' = 2Q^* - q$, and for a given $q$ we consider only those $2Q^*$ for which $2Q' > 0$.

We also consider the bubble interstitial, which consists of two particles with a relative angular momentum of 1 localized at a Thomson lattice site. Similarly to hypercorrelated interstitials, one can create hypercorrelated bubble interstitials through the attachment of additional vortices, with its wave function given by

$$\Phi^{2p,q}_{2Q,\{R\},R_B} = \prod_{j<k}^{N+1}(u_j v_k - v_j u_k)^{2p} A \left[ (J_1)^q (J_2)^q \right.$$

$$\times (u_1 v_2 - v_1 u_2)\phi^{2Q'}_{R_B}(r_1)\phi^{2Q'}_{R_B}(r_2)$$

$$\left. \times \prod_{\substack{1 \leqslant j \leqslant N-1 \\ R_j \in \{R\} \setminus \{R_B\}}} \phi^{2Q''}_{R_j}(r_{j+2}) \right], \quad (5)$$

where $R_B \in \{R\}$ is the location of the defect pair, $2Q' = 2Q^* - q(N-1) - q - 1$, and $2Q'' = 2Q^* - 2q$.

We have performed an exhaustive evaluation of energies for the vacancy, interstitial, and bubble interstitial defects in $N = 32$ and 64 particle systems, for $2p = 0, 2, 4, 6,$ and $q = 0, 1, 2$, over a wide range of filling factors using standard Markov-chain Monte Carlo techniques. To relax the CFC lattice surrounding the defect, we find it sufficient to perform a single cycle of radial relaxation; subsequent cycles only have a small effect. Remarkably, even radial relaxation causes only a very slight reduction in the defect energy for the $^{2p}$CFC, reducing the energies of vacancy and interstitial defects by no more than 20% and producing essentially no change at all for the hypercorrelated bubble defect. (In contrast, the energy of the classical centered interstitial goes from $\sim 1.48$ to $\sim 0.18$ after radial relaxation, and to 0.125 after full relaxation, with all energies in units of $e^2 \rho^{1/2}/\epsilon$.) This shows that the correlations introduced by composite fermionization automatically relax the surrounding lattice to a great degree. This also indicates that further relaxation would have a negligible impact on the CFC defect energies. We have also found that the defect energy has negligible dependence on its location on the sphere. In Fig. 2 we show density plots for certain typical relaxed bubble defects.



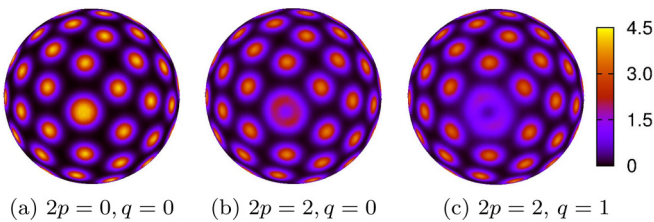(a) $2p = 0, q = 0$  (b) $2p = 2, q = 0$  (c) $2p = 2, q = 1$

FIG. 2. (Color online) Density plot of a bubble interstitial in (a) a HF crystal and (b) a CF crystal. (c) shows a hypercorrelated bubble in a CF crystal. The plots are for a system of $N = 64$ particles at $\nu = 0.21$. The number of vortices attached to every electron, $2p$, and the number of additional vortices attached to the bubble interstitial, $q$, are shown. The densities are shown in units of the average density.
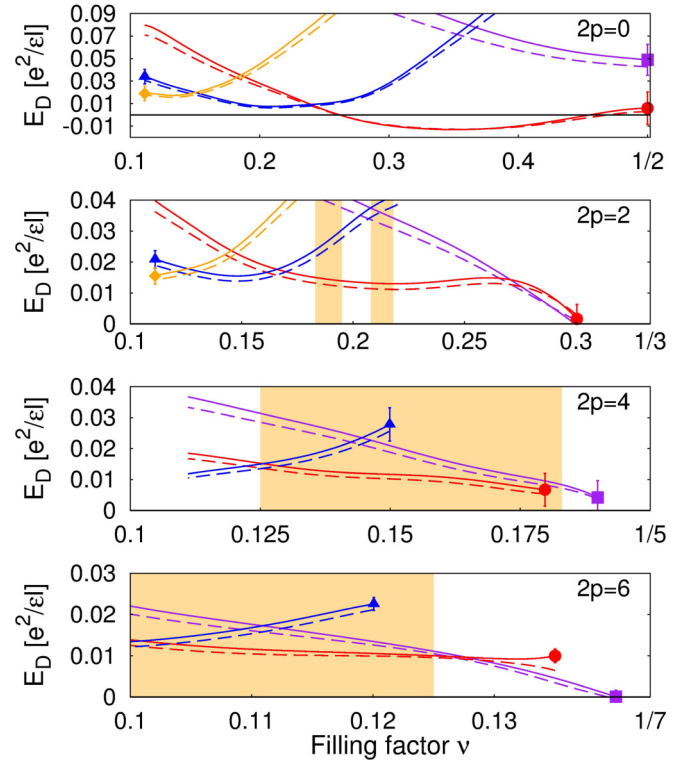


FIG. 3. (Color online) The bubble interstitial energy as a function of the filling factor for crystals of composite fermions with vorticity $2p = 0, 2, 4,$ and 6 (from top to bottom panels). Purple squares, red circles, blue triangles, and orange diamonds correspond to $q = 0$, 1, 2, and 3, respectively, where $q$ denotes the number of additional vortices attached to the bubble, as discussed in the text. The HF bubble corresponds to $2p = 0$ and $q = 0$. The shaded regions correspond to the filling factor regions where the $^{2p}$CFC under consideration is the lowest energy crystal, according to the phase diagram derived by Archer, Park, and Jain [19]. The lowest energies in the shaded regions are obtained for hypercorrelated bubbles with $q \geqslant 1$. The results are for $N = 65$ particles; error bars on each curve show the Monte Carlo statistical uncertainty in the energy.

The four panels of Fig. 3 show the energies of various defects for $2p = 0, 2, 4,$ and 6. The physically relevant region for each CFC is highlighted in yellow in each panel, according to the phase diagram of $^{2p}$CFCs evaluated previously [19]. In all cases we find, surprisingly, that the hypercorrelated $q = 1$ bubble interstitial has the lowest energy. (This is surprising because the bubble interstitial has a rather high energy in the HF crystal.) Furthermore, the energy of the hypercorrelated bubble interstitial is a factor of 3 lower than the lowest energy HF defect near $\nu = 1/5$. The energy of the bubble interstitial in $N = 64$ particle crystals is shown in Fig. 3 as a function of the filling factor. (The other defects in the CFC have a higher energy, and will be described elsewhere.) We have accounted for the finite thickness of the 2DES, indicated by the dashed lines in Fig. 3, by modifying the microscopic interaction following Shi *et al.* [32]. We have compared the bubble interstitial defect energies in $N = 32$ and 64 particles systems and found that the difference is smaller than the Monte Carlo statistical uncertainty, which leads us to believe that our

results shown in Fig. 3 are a good representation of the bubble interstitial defect energy in the thermodynamic limit.

Experiments have measured the activation energy for the crystal surrounding the $\nu = 1/5$ fractional quantum Hall (FQH) state [4–9]. They find substantial filling factor dependence of the activation energy close to 1/5, but for filling factors sufficiently far below 1/5 this energy becomes approximately constant, and is given by $0.004 \, e^2/\epsilon\ell$ in the highest mobility samples [7]. This is significantly lower than the energy of the lowest energy HF defect at $\nu = 0.18$, which is $0.028 \, e^2/\epsilon\ell$ [Fig. 1(c)]. It is in better agreement with the energy of the $q = 1$ hypercorrelated bubble defect, which has an energy of approximately $0.010 \, e^2/\epsilon\ell$ for the $^2$CF crystal surrounding the 1/5 state (Fig. 3).

A vanishing defect energy signals an instability of the crystal phase. Two kinds of instability may be seen in Fig. 3. The top panel illustrates the first type, where we see that the energy of a $q = 1$ hypercorrelated bubble in a $^0$CFC is negative for $\nu > 0.3$; this indicates that the HF state is unstable to the formation of composite fermions. The bottom three panels of Fig. 3 illustrate another type of instability, where the energy of the $q = 0$ bubble defect becomes negative as $\nu^* \to 1$ [$\nu \to 1/(2p+1)$]; this signals the transition of the $^{2p}$CFC into an FQH state.

We note that our theory does not capture the rapid decay in the activation energy upon approach to $\nu = 1/5$, as observed in experiments [7]. Such behavior is indeed not expected for a first-order transition from a crystal to liquid state. We attribute this behavior to the presence of disorder, which broadens the transition region while also converting it into a continuous one; this view is consistent with the fact that the transition region is sharpest in the highest mobility sample [7]. Narevich, Murthy, and Fertig [16] have treated the CFC in the vicinity of 1/5 with an effective Hamiltonian theory.

They find that while $^4$CFC produces low defect energies with strong $\nu$ dependence (resulting from an instability into the 1/5 FQH liquid, as explained above), the more relevant [19] $^2$CFC produces defects of much higher energy (greater than $0.1 \, e^2/\epsilon\ell$) in the vicinity of $\nu = 1/5$.

We have neglected a number of features that can have a quantitative impact on the calculated defect energy. We have not accounted for Landau-level mixing and disorder, which are expected to lead to a lowering of the gaps [33,34]. This suggests that improving sample quality should lead to even higher experimental activation energies, a trend that is apparent in the experiments of Jiang *et al.* [6,7] and Du *et al.* [9]. While these effects are beyond the scope of this Rapid Communication, it is worth noting that the discrepancy between the measured and theoretical defect energies is comparable to that between measured and theoretical gaps of the prominent FQH states, which is often attributed to a combination of Landau-level mixing and disorder [35–37].

In summary, we have shown that the quantum nature of the LLL crystal has striking implications for the defects. The lowest energy defect is a sixfold hypercorrelated bubble interstitial, the energy of which is a factor of 3 lower than the lowest defect in an uncorrelated Hartree-Fock crystal. The very low energy defects measured in experiments are thus a manifestation of the unusual quantum nature of the LLL crystal.

[1] M. C. Cross and D. S. Fisher, Rev. Mod. Phys. **57**, 881 (1985); A. J. Leggett, Phys. Rev. Lett. **25**, 1543 (1970).

[2] C. C. Grimes and G. Adams, Phys. Rev. Lett. **42**, 795 (1979).

[3] E. Y. Andrei, G. Deville, D. C. Glattli, F. I. B. Williams, E. Paris, and B. Etienne, Phys. Rev. Lett. **60**, 2765 (1988); F. I. B. Williams, P. A. Wright, R. G. Clark, E. Y. Andrei, G. Deville, D. C. Glattli, O. Probst, B. Etienne, C. Dorin, C. T. Foxon, and J. J. Harris, *ibid.* **66**, 3285 (1991); C.-C. Li, L. W. Engel, D. Shahar, D. C. Tsui, and M. Shayegan, *ibid.* **79**, 1353 (1997); Yong P. Chen, R. M. Lewis, L. W. Engel, D. C. Tsui, P. D. Ye, Z. H. Wang, L. N. Pfeiffer, and K. W. West, *ibid.* **93**, 206805 (2004).

[4] R. L. Willett, H. L. Stormer, D. C. Tsui, L. N. Pfeiffer, K. W. West, and K. W. Baldwin, Phys. Rev. B **38**, 7881 (1988).

[5] V. J. Goldman, M. Santos, M. Shayegan, and J. E. Cunningham, Phys. Rev. Lett. **65**, 2189 (1990).

[6] H. W. Jiang, R. L. Willett, H. L. Stormer, D. C. Tsui, L. N. Pfeiffer, and K. W. West, Phys. Rev. Lett. **65**, 633 (1990).

[7] H. W. Jiang, H. L. Stormer, D. C. Tsui, L. N. Pfeiffer, and K. W. West, Phys. Rev. B **44**, 8107 (1991).

[8] M. A. Paalanen, R. L. Willett, R. R. Ruel, P. B. Littlewood, K. W. West, and L. N. Pfeiffer, Phys. Rev. B **45**, 13784 (1992).

[9] R. Du, D. Tsui, H. Stormer, L. Pfeiffer, and K. West, Solid State Commun. **99**, 755 (1996).

[10] W. Pan, H. L. Stormer, D. C. Tsui, L. N. Pfeiffer, K. W. Baldwin, and K. W. West, Phys. Rev. Lett. **88**, 176802 (2002).

[11] M. B. Santos, Y. W. Suen, M. Shayegan, Y. P. Li, L. W. Engel, and D. C. Tsui, Phys. Rev. Lett. **68**, 1188 (1992).

[12] G. A. Csáthy, D. C. Tsui, L. N. Pfeiffer, and K. W. West, Phys. Rev. Lett. **92**, 256804 (2004).

[13] G. A. Csáthy, H. Noh, D. C. Tsui, L. N. Pfeiffer, and K. W. West, Phys. Rev. Lett. **94**, 226802 (2005).

[14] G. A. Csáthy, D. C. Tsui, L. N. Pfeiffer, and K. W. West, Phys. Rev. Lett. **98**, 066805 (2007).

[15] H. Yi and H. A. Fertig, Phys. Rev. B **58**, 4019 (1998).

[16] R. Narevich, G. Murthy, and H. A. Fertig, Phys. Rev. B **64**, 245326 (2001).

[17] C.-C. Chang, G. S. Jeon, and J. K. Jain, Phys. Rev. Lett. **94**, 016809 (2005).

[18] A. C. Archer and J. K. Jain, Phys. Rev. B **84**, 115139 (2011).

[19] A. C. Archer, K. Park, and J. K. Jain, Phys. Rev. Lett. **111**, 146804 (2013).

[20] D. S. Fisher, B. I. Halperin, and R. Morf, Phys. Rev. B **20**, 4692 (1979).

[21] F. D. M. Haldane, Phys. Rev. Lett. **51**, 605 (1983).

[22] J. J. Thomson, Philos. Mag. **7**, 237 (1904).

[23] D. J. Wales and S. Ulker, Phys. Rev. B **74**, 212101 (2006); D. J. Wales, H. McKay, and E. L. Altschuler, *ibid.* **79**, 224115 (2009). The minimum energy locations can be found at http://thomson.phy.syr.edu/.

[24] A. A. Koulakov, M. M. Fogler, and B. I. Shklovskii, Phys. Rev. Lett. **76**, 499 (1996).

[25] M. M. Fogler, A. A. Koulakov, and B. I. Shklovskii, Phys. Rev. B **54**, 1853 (1996).

[26] R. Price and P. M. Platzman, Phys. Rev. B **44**, 2356 (1991).

[27] E. Cockayne and V. Elser, Phys. Rev. B **43**, 623 (1991).

[28] K. Maki and X. Zotos, Phys. Rev. B **28**, 4349 (1983).

[29] J. K. Jain, Phys. Rev. Lett. **63**, 199 (1989).

[30] J. K. Jain, *Composite Fermions* (Cambridge University Press, New York, 2007).

[31] L. Zheng and H. A. Fertig, Phys. Rev. Lett. **73**, 878 (1994).

[32] C. Shi, S. Jolad, N. Regnault, and J. K. Jain, Phys. Rev. B **77**, 155127 (2008).

[33] M.-C. Cha and H. A. Fertig, Phys. Rev. Lett. **73**, 870 (1994).

[34] M.-C. Cha and H. A. Fertig, Phys. Rev. B **50**, 14368 (1994).

[35] R. R. Du, H. L. Stormer, D. C. Tsui, L. N. Pfeiffer, and K. W. West, Phys. Rev. Lett. **70**, 2944 (1993).

[36] K. Park, N. Meskini, and J. Jain, J. Phys.: Condens. Matter **11**, 7283 (1999).

[37] R. H. Morf, N. d'Ambrumenil, and S. Das Sarma, Phys. Rev. B **66**, 075408 (2002).